Finite Elements in Analysis and Design 139 (2018) 49–61

Contents lists available at ScienceDirect

Finite Elements in Analysis and Design

journal homepage: www.elsevier.com/locate/finel

Topology optimization of binary structures using Integer Linear Programming

R. Sivapuram [a,*], R. Picelli [b]

[a] *Structural Engineering, University of California, San Diego, La Jolla, CA, 92093, USA*
[b] *Cardiff School of Engineering, Cardiff University, Queen' s Buildings, 14-17, The Parade, Cardiff, CF24 3AA, United Kingdom*

A R T I C L E I N F O

Keywords:
Topology optimization
Integer Linear Programming
Relaxation
Filter
Truncation error
Compliance
Displacement constraint

A B S T R A C T

This work proposes an improved method for gradient-based topology optimization in a discrete setting of design variables. The method combines the features of BESO developed by Huang and Xie [1] and the discrete topology optimization method of Svanberg and Werme [2] to improve the effectiveness of binary variable optimization. Herein the objective and constraint functions are sequentially linearized using Taylor's first order approximation, similarly as carried out in [2]. Integer Linear Programming (ILP) is used to compute globally optimal solutions for these linear optimization problems, allowing the method to accommodate any type of constraints explicitly, without the need for any Lagrange multipliers or thresholds for sensitivities (like the modern BESO [1]), or heuristics (like the early ESO/BESO methods [3]). In the linearized problems, the constraint targets are relaxed so as to allow only small changes in topology during an update and to ensure the existence of feasible solutions for the ILP. This process of relaxing the constraints and updating the design variables by using ILP is repeated until convergence. The proposed method does not require any gradual refinement of mesh, unlike in [2] and the sensitivities every iteration are smoothened by using the mesh-independent BESO filter. Few examples of compliance minimization are shown to demonstrate that mathematical programming yields similar results as that of BESO for volume-constrained problems. Some examples of volume minimization subject to a compliance constraint are presented to demonstrate the effectiveness of the method in dealing with a non-volume constraint. Volume minimization with a compliance constraint in the case of design-dependent fluid pressure loading is also presented using the proposed method. An example is presented to show the effectiveness of the method in dealing with displacement constraints. The results signify that the method can be used for topology optimization problems involving non-volume constraints without the use of heuristics, Lagrange multipliers and hierarchical mesh refinement.

1. Introduction

The methods for structural topology optimization have been under intense research during the last couple of decades. The ultimate goal of topology optimization is to obtain binary solutions representing optimal structural layouts. The topology optimization problem can be modeled using binary variables, 0 and 1 representing the void and solid regions of the structure, respectively. This type of binary variable optimization presents an extremely challenging large-scale integer programming problem and alternatives to this formulation were proposed [4].

Towards obtaining 0/1 structures, the first widely accepted ideas considered topology optimization of continuum structures with the relaxation of binary constraint $\{0,1\}$ by using continuous density design variables [5]. This transforms the binary variable optimization problem into a density distribution problem, used in the homogenization-based method and the SIMP (Solid Isotropic Material with Penalization) method [6,7]. The SIMP model rapidly became a popular material interpolation based method with the work by Ref. [8] and his role in dissemination of the method [9]. The method was successfully applied to solve a range of important problems, such as design for nonlinear responses [10–12], stress-based design [13], design for fluid flow [14,15], dynamics design [16] and others. In such methods, gray transition material regions are intrinsically allowed between solid and void in the continuous variables definition. This leads to optimal solutions with non-explicitly defined structural boundaries and, despite their popularity, this is challenging the development of these methods in problems where explicit boundary description is important, e.g., in design-dependent multiphysics problems.

* Corresponding author.
E-mail address: rsivapur@eng.ucsd.edu (R. Sivapuram).

https://doi.org/10.1016/j.finel.2017.10.006
Received 17 July 2017; Received in revised form 13 October 2017; Accepted 24 October 2017
Available online 10 November 2017
0168-874X/

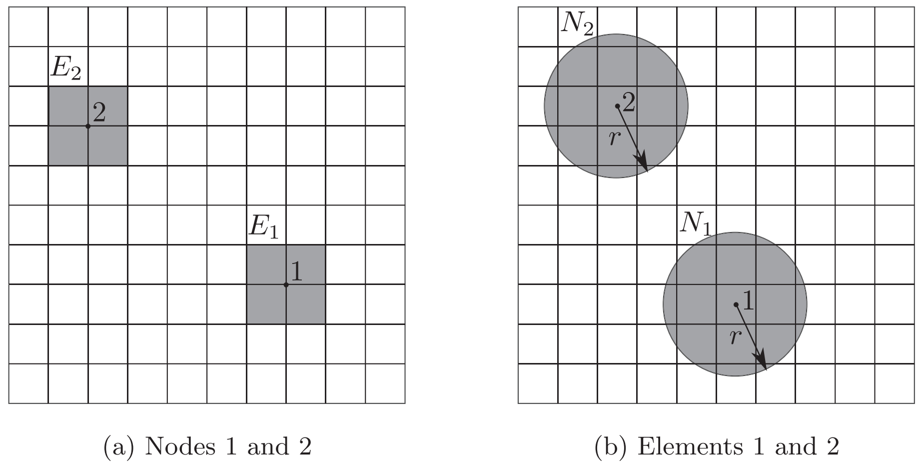

Fig. 1. Filtering - Areas of averaging for nodal and filtered elemental sensitivities.

Some researchers proposed few techniques to reduce or eliminate intermediate density (gray scale) elements in the final solutions, such as projection methods. These techniques consider Heaviside functions [17,18] or morphology-based operators [19,20] to project filtered densities into 0/1 solution space while aiming length scale control.

There are some gradient-based methods created for obtaining 0/1 optimal solutions. One class consists of boundary-description based methods, e.g. the level-set method (LSM), in which an implicit function is used to describe the structure with clearly defined boundaries. In these methods, the design variables are boundary points and shape sensitivities are derived to predict design changes [21–23]. The optimization is based on the structural shape movements and, thus, the final solution is strongly affected by the initial design configuration. A novel method with explicit boundary representation was developed by Christiansen et al. [24] with the combination of shape and topology optimization. Other class of gradient-based methods that obtain 0/1 designs employs a discrete approach, which is the focus of this paper.

The most established discrete topology optimization method is the Bi-directional Evolutionary Structural Optimization (BESO) [25]. The idea is to switch variables between void and solid using a design update scheme where sensitivities serve as indicators of the design variable performance. Although the idea was initially proposed by Xie and Steven [26], the method as it is currently used was developed by Huang and Xie [1], presenting convergent and mesh-independent solutions. Comprehensive reviews on the BESO methods are given in Refs. [27,28]. The method has been applied to a wide range of problems like nonlinear structures [29], natural frequency maximization [30,31], material optimization and multiscale problems [32–37], multiphysics problems [38,39], etc. The design variables are updated based on the thresholds of sensitivity numbers corresponding to the objective function, and the thresholds are set based on the evolutionary ratios. In this work, the use of mathematical programming enables to update the design variables without using any thresholds. Another discrete topology optimization method was proposed by Svanberg and Werme [40] where the authors effectively proposed a sequential integer linear programming approach, where one starts with a coarse mesh to solve an optimization problem and uses the final solution of this problem as the initial solution for optimization on a refined mesh and so on. They also fix a region of the structure every iteration to speed up the optimization [2]. The method proposed in this work uses a BESO filter to smoothen the sensitivities, which makes it robust and removes the need for hierarchical mesh refinement.

One more discrete structural optimization method uses Genetic Algorithms. These are derivative-free techniques based on natural selection. The design variables are genetically encoded and a pool of solutions are heuristically updated over generations [41,42]. There are too many ways of designing these algorithms and convergence is not always guaranteed. The heuristics used for cross over and selection are problem-dependent and greatly affect convergence.

While density-based methods are very well developed but do not present explicit boundaries during optimization, the BESO method showed effective potential as a binary approach such as in problems where boundary identification is important, e.g., in fluid-structure interaction problems [43]. The modern BESO method [1] updates the design variables relying on a fixed change in volume fraction every iteration, and is not based on mathematical optimization. Thus, it is not guaranteed that each iteration of BESO is an optimal step. The early ESO/BESO methods solved volume minimization problems with stress

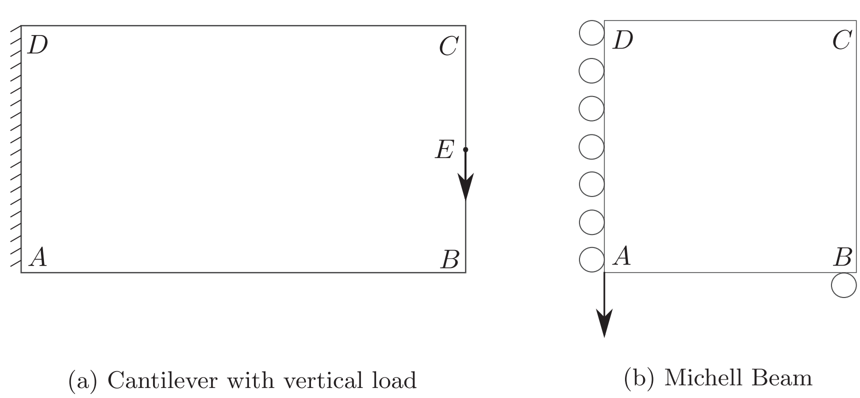

Fig. 2. Design domains and their loading configurations.

(a) Iteration 5

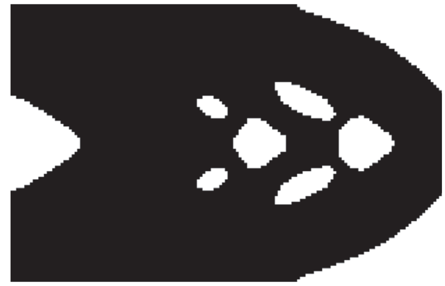

(b) Iteration 10

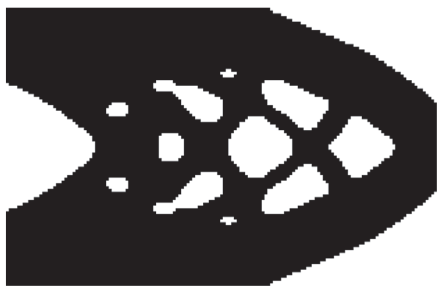

(c) Iteration 15

(d) Iteration 20

(e) Iteration 25

(f) Iteration 30

Fig. 3. Cantilever beam (Compliance Minimization subject to volume constraint) - Evolution of topologies.

(a) Optimal solution at 36 iterations

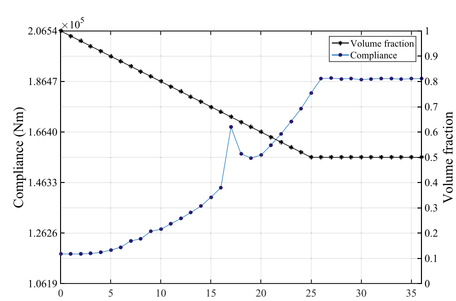

(b) Convergence History

Fig. 4. Cantilever beam (Compliance Minimization subject to volume constraint) - Optimal solution and convergence.

(a) Optimum solution at 66 iterations

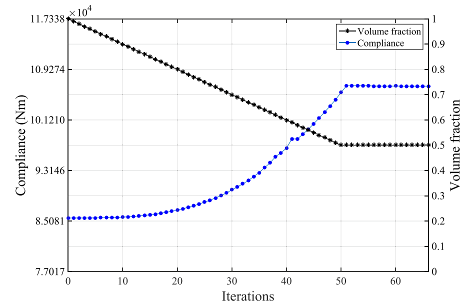

(b) Convergence History

Fig. 5. Michell beam (Compliance Minimization subject to volume constraint) - Optimal solution and convergence.

(a) Iteration 20

(b) Iteration 60

(c) Iteration 80

(d) Iteration 100

(e) Iteration 140

(f) Iteration 160

Fig. 6. Michell beam (Volume Minimization subject to compliance constraint) - Evolution of topologies.

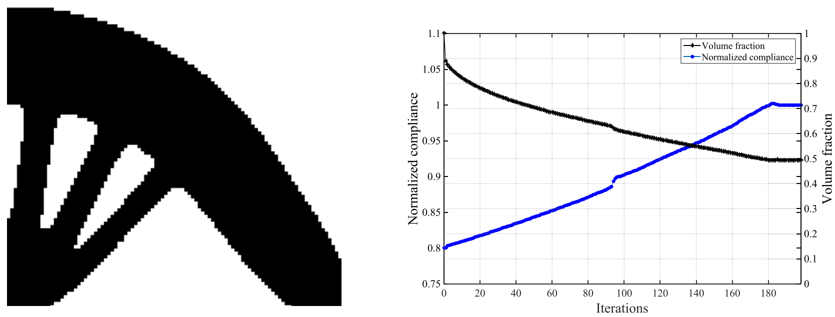

(a) Optimal solution at 197 iterations

(b) Convergence History

Fig. 7. Michell beam (Volume Minimization subject to compliance constraint) - Optimal solution and convergence.

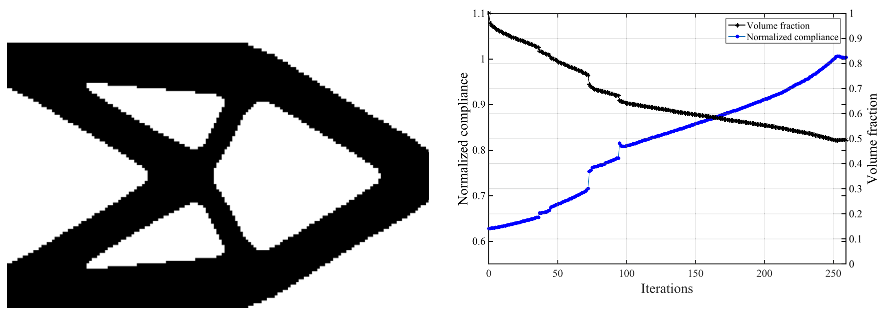

(a) Optimal solution at 258 iterations

(b) Convergence History

Fig. 8. Cantilever beam (Volume Minimization subject to compliance constraint) - Optimal solution and convergence.

[26], displacement and frequency constraints [44]. These methods are based on heuristics [3] and are non-convergent [1]. The modern BESO method uses Lagrange multipliers to deal with non-volume constraints. The selection and updating of these multipliers is not trivial. This paper aims to create an improved discrete topology optimization method by using ILP for the binary design variable updating. The objective and constraint functions are linearized using Taylor's expansion and the goal becomes to obtain the optimal change in design variables so as to improve the structural performance in each optimization step, similar to that of [2]. The maximum number of elements that can be deleted or added every iteration may be constrained to keep the truncation error low, but the optimizer is free to choose the optimal solution without exactly satisfying the constraints of linear problems. The mathematical programming allows the use of non-volume constraints explicitly, without the use of multipliers. Herein, the sensitivity analysis is similar to that of BESO. Any method of sensitivity analysis can be used as long as only the extreme values 0/1 are obtained by design variable updating. In the proposed method, a soft-kill approach of elements and extrapolation of sensitivities to void regions by filtering are used.

The remainder of the paper is organized as follows. Section 2 describes the formulation and implementation details of the proposed method. The linearization of a generic binary variable optimization problem and the relaxation of constraints is given in subsection 2.1. The details of ILP implementation are discussed in subsection 2.2. The description of sensitivity analysis is presented in subsection 2.3 and sensitivity filtering is given in subsection 2.4. Section 3 presents the various steps used for the proposed method of discrete topology optimization using ILP. Section 4 shows the results obtained by using the proposed method for compliance minimization problems (subsection 4.1)

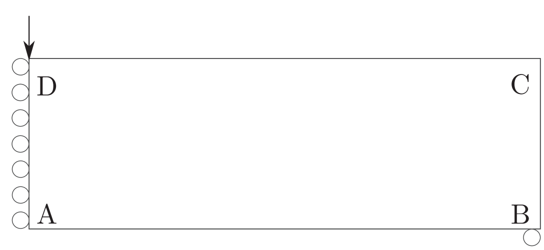

Fig. 9. MBB beam - Design domain and loading configuration.

and compliance constrained problems (subsection 4.2). Volume minimization subject to compliance constraint in design-dependent fluid pressure loading problems is also investigated, and the results are discussed. Compliance minimization subject to volume and displacement constraints is also presented (subsection 4.3) to demonstrate effectiveness of the method for different displacement constraint values. Section 5 presents the summary and key contributions of the work.

2. Proposed methodology

2.1. Problem linearization

The proposed method uses binary design variables, one for each of the finite elements in the mesh of a structural domain, similar to that of BESO. The design variable 1 implies the finite element is filled with material, 0 indicates void. Consider an objective function $f(\mathbf{x})$, constrained by $g_i(\mathbf{x}) \leq \overline{g}_i$. $i \in [1, N_g]$, with $\mathbf{x}$ being the design variables. The

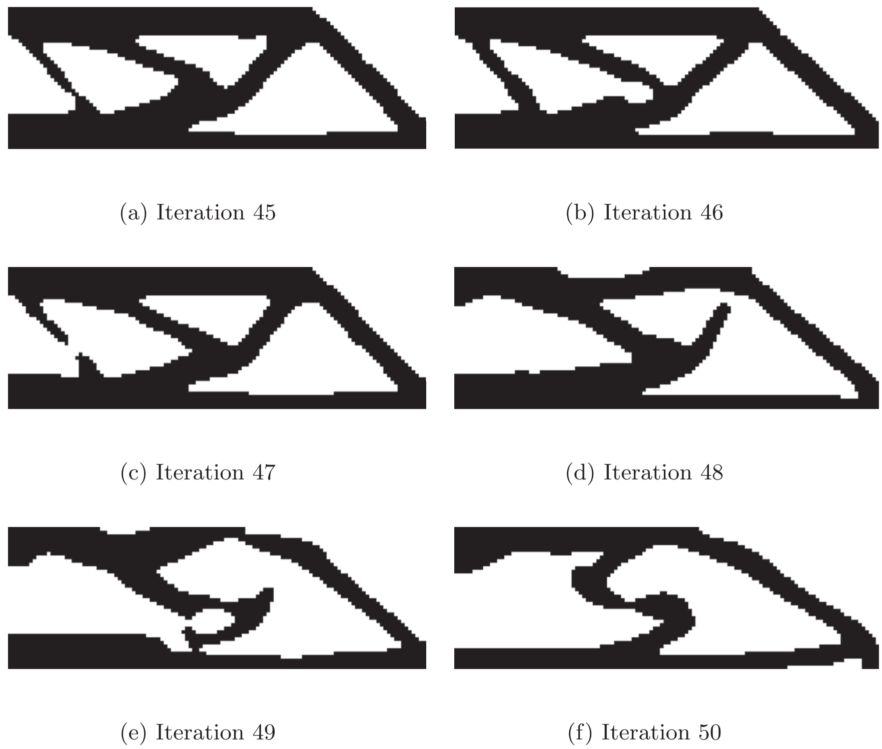

Fig. 10. MBB Beam (Volume minimization subject to compliance constraint - Oscillations during the evolution of topologies).

binary variable optimization problem can be formulated as follows:

$$\begin{aligned} &\underset{\mathbf{x}}{\text{Minimize}} && f(\mathbf{x}) \\ &\text{Subject to} && g_i(\mathbf{x}) \leq \overline{g}_i \quad i \in [1, N_g] \\ & && x_j \in \{0, 1\} \quad j \in [1, N_d] \end{aligned} \tag{1}$$

where N_d is the number of design variables, i.e., the number of finite elements in the mesh. Using first order Taylor's approximation, (1) can be converted into a linearized form as shown in (2).

$$\begin{aligned} &\underset{\Delta\mathbf{x}^k}{\text{Minimize}} && \left.\frac{\partial f}{\partial \mathbf{x}}\right|_{\mathbf{x}^k} \Delta\mathbf{x}^k \\ &\text{Subject to} && \left.\frac{\partial g_i}{\partial \mathbf{x}}\right|_{\mathbf{x}^k} \Delta\mathbf{x}^k \leq \overline{g}_i - g_i^k \quad i \in [1, N_g] \\ & && \Delta x_j \in \{-x_j, 1 - x_j\} \quad j \in [1, N_d] \end{aligned} \tag{2}$$

where g_i^k is the value of constraint g_i at iteration k of optimization. After each iteration, the design variables are updated as shown in (3).

$$\mathbf{x}^{k+1} = \mathbf{x}^k + \Delta\mathbf{x}^k \tag{3}$$

We can see from the optimization problem (2) that the formulation is generic and can be used for problems involving any type of constraints. The binary linear optimization problem in (2) can be solved using ILP.

The linearization approximation is valid only for small changes in the objective and constraint functions at every iteration. To achieve this, we use a relaxation scheme on targets $\overline{g}_i$ of the constraints such that the differences between the constraint targets and the current values of constraints are small. This also ensures that the ILP has a feasible solution. Whenever g_i^k is away from $\overline{g}_i$, we use a constraint target relaxation specified in (4).

$$\Delta g = \begin{cases} -\epsilon_1 g^k & : \overline{g} < (1 - \epsilon_1) g^k \\ \overline{g} - g^k & : \overline{g} \in [(1 - \epsilon_1) g^k, (1 + \epsilon_2) g^k] \\ \epsilon_2 g^k & : \overline{g} > (1 + \epsilon_2) g^k \end{cases} \tag{4}$$

where g is any of the N_g constraints, and Δg is the right hand side of the constraint which is relaxed from $\overline{g} - g^k$ at iteration k. The parameters ϵ_1, ϵ_2 are chosen such that ILP has a feasible solution. They are usually small numbers so as to maintain the linearization valid. Any other definition for relaxation can be used as long as the constraints are relaxed in a similar way as shown in (4).

There are many methods in literature where an optimization problem is solved by sequentially solving simpler approximate problems. Griffith and Stewart [45] proposed sequential linear programming where linearization is used to create subproblems. Svanberg [46] used a nonlinear convex approximation for creating subproblems. Sequential Quadratic Programming (SQP) uses quadratic approximate subproblems which account for curvature of the functions due to which saddle point solutions are avoided [47]. Other methods like [48] use the same idea of linearization to create subproblems.

2.2. Integer linear programming

An integer programming problem is a linear programming problem with the additional restriction that the feasible space of solutions is the integer space. Branch and bound algorithm is a famous technique used to solve an ILP. The technique initially solves the ILP as a Linear Program (LP), i.e., without any integer restraints. The solution obtained is used as the initial solution and different LPs are solved adding extra bounds on the design variables which force the optimizer to yield integer solutions in the branches. In general, the computational complexity


(a) Iteration 0 (b) Iteration 20


(c) Iteration 38 (d) Iteration 42


(e) Iteration 60 (f) Iteration 80

Fig. 11. MBB Beam (Volume Minimization subject to compliance and volume addition and removal constraints) - Evolution of topologies.

(a) Optimal solution at 99 iterations

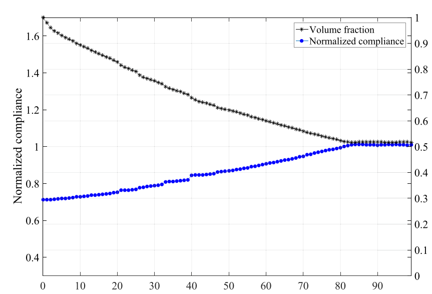

(b) Convergence History

Fig. 12. MBB beam (Volume Minimization subject to compliance and volume addition and removal constraints) - Optimal solution and convergence.

of an ILP problem is higher than that of an LP problem [49].

In this work, we used the `intlinprog` function of MATLAB for solving ILP problems. We used some options in the optimizer to ensure better performance. While solving an ILP problem, additional constraints called cuts are imposed by the optimizer to restrict the feasible space to integer solutions. The `CutGeneration` option is set to `intermediate` which uses the most cut types [50]. Primal-Simplex algorithm is used for solving the LP problems formed in branches of the optimizer. The number of nodes searched by the branch and bound method of ILP `HeuristicsMaxNodes` is chosen to be 100. The decision on whether a design variable enters the basis is taken by checking if the reduced cost corresponding to the design variable exceeds a tolerance. This tolerance is set in the `LPOptimalityTolerance` option to 10^{-10}. These options yielded better performance of ILP over a wide range of problems.

2.3. Sensitivity analysis

In this paper, we focused on solving problems related to linear elasticity with compliance and volume as either objective or constraint functions. If C is the compliance of a structure with design-independent loads, the sensitivity with respect to design variable x_j is given by (5).

$$\frac{\partial C}{\partial x_j} \approx -\frac{1}{2}\mathbf{u}_j^T \mathbf{K}_j^e \mathbf{u}_j \tag{5}$$

where $\mathbf{K}_j^e$ is the stiffness matrix corresponding to solid finite element j, and $\mathbf{u}_j$ is the displacement vector corresponding to finite element j. In this work, we have used the soft-kill approach, i.e., the void elements are assembled in finite element analysis using $x_j = 0.001$, to prevent singularity of the global stiffness matrix $\mathbf{K}$. We also observed that the oscillations in topology optimization are reduced by using the soft-kill approach. The sensitivity of volume V of the structure with respect to

Fig. 13. Cantilever beam - Initial Solution.

design variable x_j is shown in (6).

$$\frac{\partial V}{\partial x_j} \approx V_j \tag{6}$$

where V_j is the volume of finite element j. In this work, unit-sized finite elements are used in topology optimization, i.e., $V_j = 1,\ \forall j \in [1, N_d]$. We also presented topology optimization of a structure with design-dependent fluid pressure loads [51]. The sensitivity of compliance with respect to design variable x_j is given by (7).

$$\frac{\partial C}{\partial x_j} \approx -\frac{1}{2}\mathbf{u}_j^T \mathbf{K}_j^e \mathbf{u}_j + \mathbf{u}_j^T \Delta \mathbf{L} \mathbf{P}_f \tag{7}$$

where $\mathbf{P}_f$ is the fluid pressure in the fluid finite element which shares boundary with the solid finite element j, and $\Delta\mathbf{L} = \mathbf{L}^* - \mathbf{L}$ is a semi-analytical sensitivity of the fluid-solid coupling matrix, where $\mathbf{L}$ and $\mathbf{L}^*$ are the fluid-solid coupling matrices obtained before and after changing the solid element j to fluid.

When an inequality constraint is applied on a displacement degree of freedom in the structure (Equation (8)), we solve an adjoint problem for computing the sensitivities.

$$d \le \overline{d} \tag{8}$$

The adjoint problem and sensitivity of the displacement constraint (8) with respect to x_j are given by:

$$\begin{aligned} \mathbf{K}\lambda + \mathbf{H} &= 0 \\ \frac{\partial d}{\partial x_j} &\approx \lambda_j^T \mathbf{K}_j^e \mathbf{u}_j \end{aligned} \tag{9}$$

where λ is the vector of adjoint variables, and has the same size as that of the global displacement vector $\mathbf{u}$, $\mathbf{H}$ is the vector having only one non-zero entry 1 at the location corresponding to displacement d and λ_j is the vector of adjoint variables corresponding to finite element j.

2.4. Sensitivity filter

The sensitivities need to be filtered to make sure the existence of solutions. Filtering is also required to obtain non-checkerboard and mesh-independent optimal solutions [28]. A nodal sensitivity field is created from the design variable sensitivities, by averaging the sensitivities corresponding to finite elements attached to the nodes. Fig. 1a shows nodes 1 and 2 and the corresponding finite element regions E_1 and E_2 whose sensitivities are used for averaging at the nodes. The nodal sensitivity (with respect to a virtual nodal design variable y_n) at a node n is calculated as shown in (10).

$$\frac{\partial C}{\partial y_n} = \frac{1}{|E|}\sum_{e \in E} \frac{\partial C}{\partial x_e} \tag{10}$$

where E is the set of finite elements having n as a node, and $|E|$ is the number of such elements. The filtered sensitivity field with respect to the density design variables is reconstructed from the nodal sensitivity field by using weighted-distance averaging in a neighborhood of each finite element. Fig. 1b shows the filtering regions N_1 and N_2 whose nodal sensitivities are used for averaging to compute the filtered sensitivities for elements 1 and 2. The filtered sensitivity with respect to density x_j is computed as shown in (11).

$$\widetilde{\frac{\partial C}{\partial x_j}} = \frac{\sum_{i \in N} w_{ji} \frac{\partial C}{\partial y_i}}{\sum_{i \in N} w_{ji}} \tag{11}$$

where N is the set of nodes in a neighborhood of the element j. In this work, we use a circular neighborhood of radius r with the center being the centroid of finite element j for filtering, and $w_{ji} = \mathtt{max}(0, r - \mathtt{dist}(j,i))$, with $\mathtt{dist}(j,i)$ being the distance between centroid of finite element j and node i.

3. Steps in the proposed method

This section presents the algorithmic steps for the proposed method.

1. Consider the topology optimization of a structure. Discretize the design domain, apply loads and boundary conditions. The model can be reduced if any symmetry is present.
2. Choose the parameters like ϵ_1 and ϵ_2 (based on the general range of constraint values), β_a, β_r, filter radius r and convergence criteria.
3. Perform Finite Element Analysis (FEA) for the structure and compute sensitivities for the objective function and constraints with respect to the design variables $\mathbf{x}$ using (5)–(7) and (9), etc. The values of the objective and constraint functions are calculated.
4. Filter the sensitivities for each function (volume sensitivities need not be filtered since they are uniform for a uniform mesh) using the details presented in subsection 2.4.
5. The constraints are relaxed so that the structure does not change very much using (4).

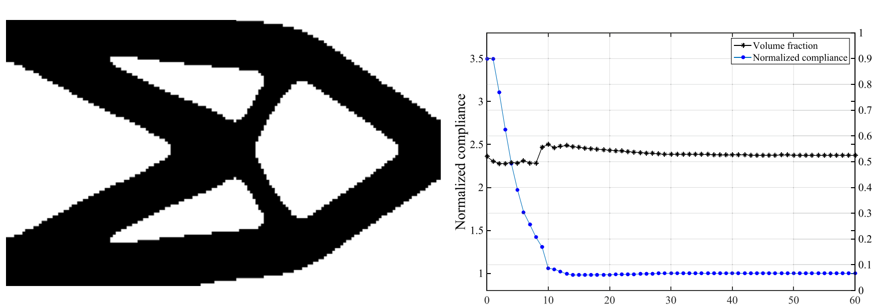

(a) Optimal solution at 60 iterations

(b) Convergence History

Fig. 14. Cantilever beam (Volume Minimization subject to compliance and volume addition and removal constraints) - Optimal solution and convergence.

6. Some extra constraints to restrain the maximum number of elements added and removed may be used, as described in subsection 4.2.
7. The filtered sensitivities are supplied to ILP and the optimization problem (2) is solved after replacing the right hand side of constraints with the relaxed constraint targets. The optimal change in design variables is computed.
8. The design variables are updated using (3).
9. The structure generated using the updated design variables is tested for convergence. If convergence is achieved, continue to post-processing, otherwise go to step 3.
10. Post-processing like plotting the optimized structure and convergence of the functions is finally done.

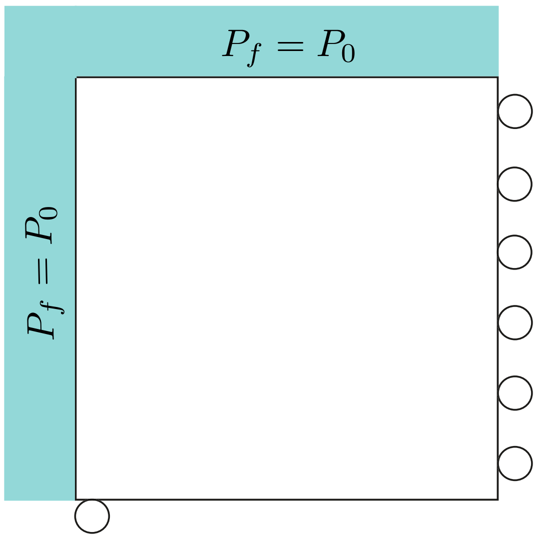

Fig. 15. Design domain with fluid pressure loading.

4. Examples

This section aims to demonstrate the performance of the method proposed in this work. First, it is shown that volume constraints used in the standard BESO are well accommodated in the present methodology. Different examples of volume minimization subject to compliance constraints are then used to demonstrate the flexibility of the method in dealing with non-volume constraints. An example is presented for minimizing the volume subject to compliance constraints when the structure is subjected to design-dependent loads. Finally, the effectiveness of the method in dealing with displacement constraints is explored.

4.1. Compliance minimization subject to volume constraints

We present some examples of topology optimization for minimizing compliance with volume being constrained. Fig. 2 shows the examples considered for topology optimization. Fig. 2a shows a cantilever beam (1.6 : 1 aspect ratio) *ABCD* with a unit vertical load applied at Point *E* on the right edge *BC*. Due to symmetry, only the lower half of design

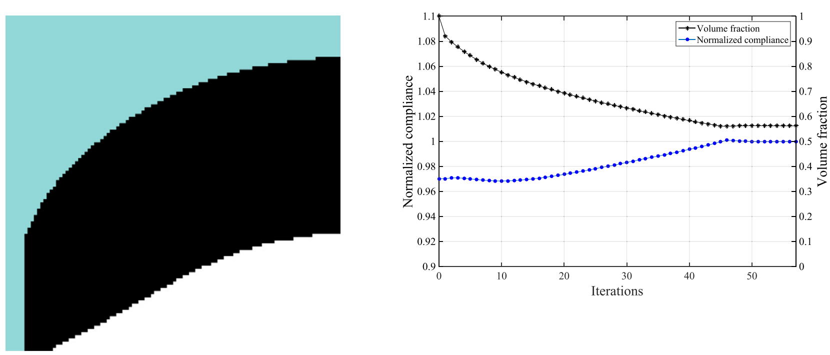

(a) Optimal solution at 57 iterations (b) Convergence History

Fig. 16. Arch-like structure (Volume Minimization subject to compliance (5 Nm) and volume addition and removal constraints) - Optimal solution and convergence.

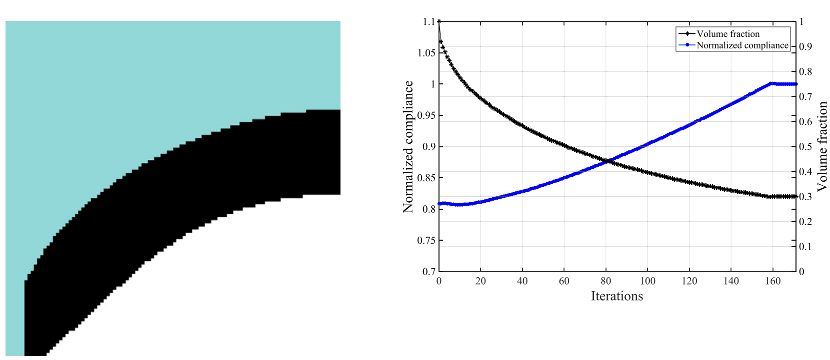

(a) Optimal solution at 170 iterations (b) Convergence History

Fig. 17. Arch-like structure (Volume Minimization subject to compliance (6 Nm) and volume addition and removal constraints) - Optimal solution and convergence.

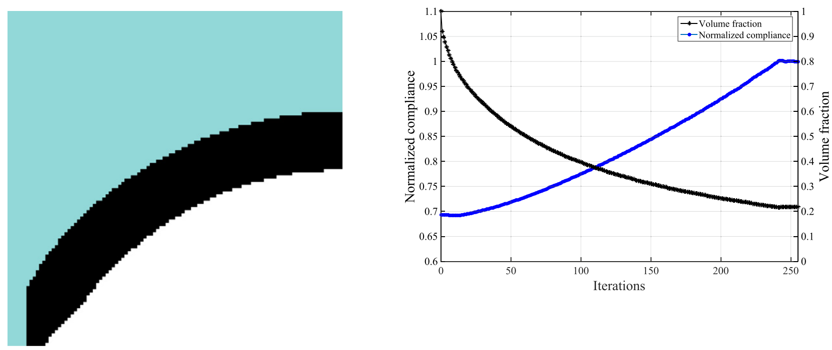

(a) Optimal solution at 256 iterations (b) Convergence History

Fig. 18. Arch-like structure (Volume Minimization subject to compliance (7 Nm) and volume addition and removal constraints) - Optimal solution and convergence.

domain is considered for optimization. Fig. 2b shows the symmetric portion of a Michell beam (2 : 1 aspect ratio) *ABCD* with a unit point vertical load applied at *A*. The design domains are well-supported to avoid rigid body motions. The Young's Moduli of the solid and void finite elements are 1.0 and 0.001 respectively, while the Poisson's ratio is 0.3 for both types of elements. The cantilever design domain in Fig. 2a is discretized using 160×100 bilinear quadrilateral finite elements.

Topology optimization requires an initial solution to start iterating so as to find a local optimal solution. A design domain completely filled with solid finite elements is used as the initial guess for optimization. The upper bound on volume fraction is 0.5 in both the examples. We used $\epsilon_1 = \epsilon_2 = 0.01$, $r = 6$ for the cantilever beam and $r = 3$ for the Michell structure in terms of number of finite elements. Few topologies during the evolution of cantilever beam are shown in Fig. 3. We can observe that the regions near Points *B* and *C* become void at the very early stages of evolution because these regions experience negligible strains. Members are formed inside the structure to keep the compliance low while deleting some material to achieve the volume constraint. Fig. 4 shows the optimum structure obtained after 36 iterations and the convergence history. We can observe that both the objective and constraint functions converge smoothly.

The Michell beam design domain in Fig. 2b is discretized using 100×100 bilinear quadrilateral elements. Fig. 5 shows the optimum structural design and convergence history of the Michell beam. The convergence is achieved at 66 iterations and both compliance and volume fraction converge smoothly.

These examples demonstrate that the proposed method yields good results for compliance minimization with volume constraint similar to that of BESO, by using ILP instead of sensitivity number thresholds. The only parameters in this algorithm are ϵ_1, ϵ_2 which are used for relaxing the constraints thereby creating feasible points for ILP, and r for sensitivity filtering. The method produces good solutions directly using fine meshes, unlike [2] who used hierarchical mesh refinement.

4.2. Volume minimization subject to compliance constraints

The design domains in Fig. 2a and b are considered for minimization of volume subject to compliance constraint. The design domains completely filled with solid finite elements are used as the initial solutions. The parameters chosen are $\epsilon_1 = \epsilon_2 = 0.0005$, $r = 5$ and $r = 3$ finite elements for the cantilever and Michell problems respectively.

The upper bound of compliance for the Michell beam topology optimization is 10.7×10^4 Nm. Fig. 6 shows few topologies during the evolution of Michell beam. At the beginning of evolution, the finite elements near Point *C* are subject to negligible strains. These finite elements get deleted at an early stage of optimization. Members are formed

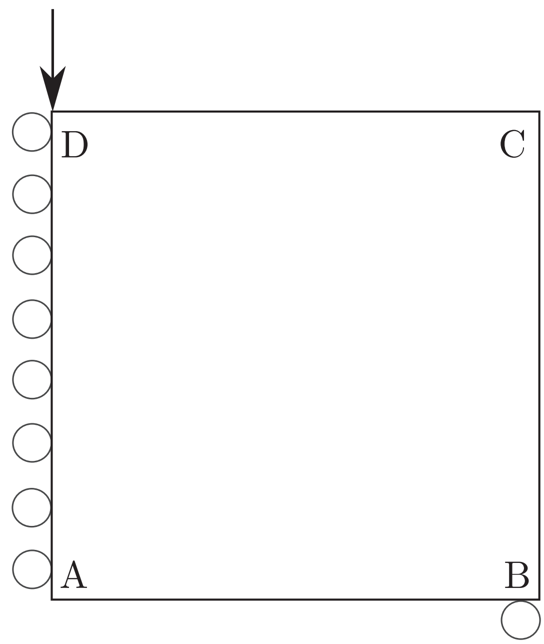

Fig. 19. Design domain and boundary conditions [53].

in the structure over iterations to improve the objective (volume) while satisfying the inequality constraint (compliance). Fig. 7 shows the optimal solution obtained after 197 iterations and the convergence history. We can see that convergence of the objective and constraint functions is smooth for this compliance-constrained problem. We can also observe that since the compliance constraint chosen is the optimal compliance value from the compliance minimization of Michell structure (5), the optimal volume fraction of the current volume minimization problem is equal to the volume fraction constraint of the former problem, i.e, 0.5. This demonstrates that the method is capable of reproducing structures obtained through compliance minimization, even when compliance is used as a constraint.

Fig. 8 shows the optimal structure and convergence history for the volume minimization of cantilever beam, with an upper bound on compliance at 1.88×10^5 Nm. We can observe the optimal structure obtained looks similar to that obtained in the compliance minimization example (Fig. 4). The optimal cantilever obtained in the compliance minimization case has an objective of 1.88×10^5 Nm and a volume fraction of 0.5. We can observe that the volume fraction of optimal structure for the volume minimization problem is 0.5. This means that equivalent structures are obtained by changing the roles of compliance and volume fraction between objective and constraint functions.

Fig. 9 shows the symmetric portion of design domain of a Messerschmitt-Bölkow-Blohm (MBB) beam with a unit vertical load applied at point D. The design domain is constrained to prevent any rigid body motions. The Young's modulus is 1.0 and Poisson's ratio is 0.3 for a solid finite element. The void elements are dealt using the soft-kill approach. The design domain is discretized using 120×40 finite elements. The parameters used are $\epsilon_1 = \epsilon_2 = 0.001$, $r = 4$ finite elements, and the upper bound on compliance used is 9×10^5 Nm.

Fig. 10 shows few topologies during the evolution of the compliance-constrained MBB beam. It is observed that the evolution is noisy with large volumes of material removed and added every iteration after 45th iteration. The members in the structure also oscillate creating a noisy evolution.

The parameters ϵ_1, ϵ_2 relax the constraints, i.e., allow the constraint (here compliance) to vary by a small amount each iteration. They do not restrict the amount of volume removed and added each iteration. This could make the truncation error of linearization larger, making the linear approximations erroneous. The volume of the material removed and added at every iteration needs to be constrained so as to keep the truncation error ($O(\|\Delta\mathbf{x}\|_2^2)$) low. To achieve this, we introduce extra constraints on the removal and addition of material every iteration. The constraints are given by (12).

$$\begin{aligned} &\sum_{i \in V} \Delta x_i \leq \beta_a N_d \quad V = \{i | x_i^k = 0\} \\ &\sum_{i \in S} \Delta x_i \geq -\beta_r N_d \quad S = \{i | x_i^k = 1\} \end{aligned} \tag{12}$$

where β_a and β_r are positive fractions and restrain the number of design variables that are allowed to be removed and added from the structure respectively. The sets V and S consist of the indices of finite elements which are void and solid in the current iteration k respectively.

The MBB beam is re-optimized to minimize volume subject to compliance constraint and the additional constraints (12) to restrict the removal and addition of material every iteration. The fractions used are $\beta_a = \beta_r = 0.02$.

Fig. 11 shows few topologies during evolution of the optimal structure. In the initial iterations, the regions with negligible strains like the regions near Point C and midpoint of edge AD become void. Structural members begin to form to minimize the volume while maintaining the relaxed compliance constraint at every iteration. We can see that the topologies evolve smoothly after adding the extra constraints. Fig. 12 shows the optimal structure of the MBB beam obtained after 99 iterations and the convergence history. We can observe that the objective and constraint functions converge smoothly. The addition of β_a and β_r has similar goals as that of $AR_{\max}$ and ER parameters of the BESO method, with a small difference that the target volume fraction is pre-decided every iteration in BESO, while the maximum number of elements getting added and deleted every iteration is constrained using β_a and β_r in the current method [52]. developed a connectivity constraint for discrete topology optimization methods based on an associativity matrix which describes the connectivity between active elements. The connectivity of the structure can be controlled by changing the target connectivities of active elements in the structure.

The volume minimization of cantilever beam subject to compliance constraint of 1.8×10^5 Nm is performed and the initial design used is shown in Fig. 13. The white part signifies the void region and black part corresponds to the material in the structure. The parameters used are $\epsilon_1 = \epsilon_2 = 0.001$, $r = 6$ finite elements, $\beta_a = \beta_r = 0.2$. The optimal structure obtained after 60 iterations and the convergence history is shown if Fig. 14. We can observe that the functions have a smooth convergence. This example also demonstrates the robustness of the method by using an initial solution different from the fully filled design domain.

Fig. 15 shows the symmetric portion of a design domain (2 : 1

(a) $d_B \leq 1.4$mm

(b) $d_B \leq 1.2$mm

(c) $d_B \leq 1.0$mm

Fig. 20. Optimum solutions for compliance minimization subject to displacement and volume constraints.

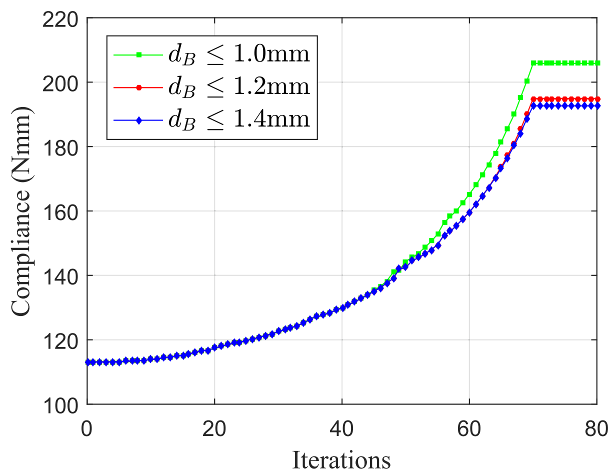

Fig. 21. Convergence of Compliances for the three cases of displacement constraints.

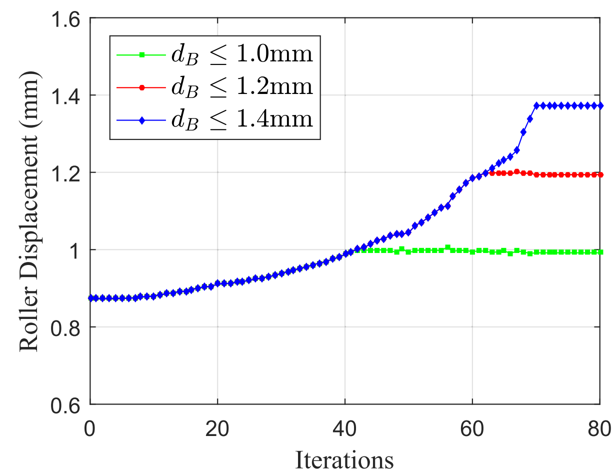

Fig. 22. Convergence of displacement constraints for the three cases.

aspect ratio) surrounded by a fluid with constant pressure P_0. The design domain is discretized using a mesh of 100×100 bilinear quadrilateral elements. The design domain is subjected to volume minimization and a compliance constraint. The parameters used are $\epsilon_1 = \epsilon_2 = 0.001$, $r = 4$ finite elements, $\beta_a = \beta_r = 0.1$. The fully solid structure is used as the initial design for topology optimization.

Figs. 16–18 show the optimal structures and convergence histories of the volume minimization when the upper bounds used on compliance are 5 Nm, 6 Nm and 7 Nm respectively. In all three cases, arch-like structures are created which are optimal for bearing design-dependent fluid pressure loads [51]. As the upper bound on compliance increases, the thickness of the arch decreases due to the removal of more material from the structure. We can clearly observe that the compliance and volume fraction converge smoothly in the three cases. This example demonstrates that the proposed method works well for compliance constraints in problems with design-dependent loads.

4.3. Compliance minimization subject to a displacement constraint

This example [53] is a compliance minimization problem subject to volume and displacement constraints, when a unit point vertical load is acting on the structure. Due to symmetry, only half of the model (50 mm × 50 mm) is considered for optimization, as shown in Fig. 19. The Young's Modulus of the material is 1.0 GPa and the Poisson's ratio is 0.3. A 100×100 mesh of bilinear quadrilaterals is used to discretize the geometry. The upper bound on volume fraction of the structure is 0.3. We consider three problem cases where horizontal displacement at Point B is constrained to be 1.4 mm, 1.2 mm and 1.0 mm respectively. The parameters used are $\epsilon_1 = \epsilon_2 = 0.01$ for the volume constraint, $\epsilon_1 = \epsilon_2 = 0.25$ for the displacement constraint, $\beta_a = \beta_r = 0.05$ and $r = 3$ finite elements.

Fig. 20 shows the optimal topologies obtained when the horizontal displacement at point B d_B is constrained to be below 1.4 mm, 1.2 mm and 1.0 mm. The compliance of the optimal solutions is 192.63 Nmm, 194.95 Nmm and 205.83 Nmm respectively. Fig. 21 shows the convergence of compliances. We can observe that the convergence is smooth in all the three cases. The optimal topologies have features similar to that of [53], and the compliance values of the optimal solutions are comparable. This example demonstrates the effectiveness of the method for problems with a displacement constraint.

[53] use a Lagrange multiplier approach for dealing with the displacement constraint, so as to modify the topology optimization problem to optimization of an objective function subject to volume constraint. The choice of Lagrange multiplier used for the constraint and its updating is not trivial. The Lagrange multiplier is non-zero only when the inequality displacement constraint is not satisfied. When the constraint is just satisfied near convergence, the Lagrange multiplier switches to zero and the problem becomes a compliance minimization problem subject to volume constraint. This allows the optimizer to minimize compliance without any regard to d_B at that iteration, thereby potentially failing to satisfy the displacement constraint. This may also lead to an oscillatory convergence of the displacement constraint. In this work, the constraints are handled explicitly, i.e., no Lagrange multipliers or penalty-based methods are used. Fig. 22 shows the convergence of displacement constraint for the three cases. The convergence of the constraints is smooth, because the constraint does not get removed from optimization even when it is satisfied. Thus the optimizer minimizes compliance without violating the displacement constraint. This example demonstrates that the method proposed in this work is capable of handling the non-volume constraints without the use of any Lagrange multipliers.

5. Conclusions

A discrete method is proposed for topology optimization of structures to obtain binary (void (0) and solid (1)) designs. The proposed method uses sequential linear approximations of the objective and constraint functions to obtain integer linear problems, solved using Integer Linear Programming (ILP). The proposed method uses mathematical programming for design variable updating, unlike the BESO method. This helps the method to accommodate non-volume constraints explicitly, unlike the modern BESO method which uses Lagrange multipliers. The present method is also mesh-independent because of the use of mesh-independency filter taken from the modern BESO method [1]. The method does not require any hierarchical mesh refinement during optimization, unlike Svanberg and Werme [2]. A soft-kill approach is used for dealing with the void elements so as to obtain a positive definite global stiffness matrix for the model. A constraint relaxation method is used to allow only small changes in the constraint functions each iteration thereby assuring the existence of feasible solutions for ILP. Few examples are demonstrated for compliance minimization subject to volume constraint. The results demonstrate that the proposed method works well in the same way as BESO method for compliance minimization problems. Some examples are solved for volume minimization subject to compliance constraint, and the results show smooth convergence to optimal structures. We observed oscillations in evolving topologies because of the unrestrained removal and addition of material every iteration. This is overcome by constraining the removal and addition of material during optimization. The results have shown clear topologies with nice convergence. Volume minimization subject to compliance constraint is also solved in problems with design-dependent fluid pressure loading for different upper bounds on compliance. In all cases, nice arch-like structures are created in the optimal solution with smooth convergence. We also demonstrated effectiveness of the method for a compliance minimization problem subject to volume and displacement constraints. The proposed method obtains smooth convergence of the displacement constraint because the constraint is not dealt using Lagrange multiplier. Parameters are required in the proposed method for constraint relaxation, filtering and for restraining addition and removal of material every iteration. The proposed method has the potential to deal with non-volume constraints without using heuristics, Lagrange multipliers or hierarchical mesh refinement, which is a significant improvement over the existing discrete topology optimization methods (like the early ESO/BESO, the modern BESO, discrete topology optimization by Ref. [2]). The current work demonstrates topology optimization with compliance and displacement constraints. The application of the method to other types of constraints and to microstructural optimization is a work for the future.

References

[1] X. Huang, Y.M. Xie, Convergent and mesh-independent solutions for the bi-directional evolutionary structural optimization method, Finite Elem. Anal. Des. 43 (2007) 1039–1049.
[2] K. Svanberg, M. Werme, Topology Optimization by Sequential Integer Linear Programming, Springer Netherlands, Dordrecht, 2006, ISBN: 978-1-4020-4752-7., pp. 425–436, https://doi.org/10.1007/1-4020-4752-5_42.
[3] G.I.N. Rozvany, A critical review of established methods of structural topology optimization, Struct. Multidiscip. Optim. 37 (2009) 217–237.
[4] J.D. Deaton, R.V. Grandhi, A survey of structural and multidisciplinary continuum topology optimization: post 2000, Struct. Multidiscip. Optim. 49 (2014) 1–38.
[5] M.P. Bendsøe, N. Kikuchi, Generating optimal topologies in structural design using a homogenization method, Comput. Methods Appl. Mech. Eng. 71 (1988) 197–224.
[6] G.I.N. Rozvany, M. Zhou, T. Birker, Generalized shape optimization without homogenization, Struct. Optim. 4 (1992) 250–254.
[7] M.P. Bendsøe, O. Sigmund, Topology Optimization - Theory, Methods and Applications, Springer Verlag, Berlin Heidelberg, 2003.
[8] O. Sigmund, Design of Material Structures Using Topology Optimization, Ph.D. thesis, Department of Solid Mechanics, Technical University of Denmark, 1994.
[9] O. Sigmund, Design of multiphysics actuators using topology optimization - Part I: one material structures, Comput. Methods Appl. Mech. Eng. 190 (2001) 6577–6604.
[10] T. Buhl, C.B. Pedersen, O. Sigmund, Stiffness design of geometrically non-linear structures using topology optimization, Struct. Multidiscip. Optim. 19 (2) (2000) 93–104.
[11] T.E. Bruns, D.A. Tortorelli, Topology optimization of non-linear elastic structures and compliant mechanisms, Comput. Methods Appl. Mech. Eng. 190 (26–27) (2001) 3443–3459.
[12] G.H. Yoon, Y.Y. Kim, Element connectivity parameterization for topology optimization of geometrically nonlinear structures, Int. J. Solids Struct. 42 (7) (2005) 1983–2009.
[13] C. Le, J. Norato, T. Bruns, C. Ha, D. Tortorelli, Stress-based topology optimization for continua, Struct. Multidiscip. Optim. 41 (2010) 605–620.
[14] T. Borrvall, J. Petersson, Topology optimization of fluids in Stokes flow, Int. J. Numer. Methods Fluids 41 (2003) 77–107.
[15] G.H. Yoon, Topology optimization for stationary fluid-structure interaction problems using a new monolithic formulation, Int. J. Numer. Methods Eng. 82 (2010) 591–616.
[16] J. Du, N. Olhoff, Topological design of freely vibrating continuum structures for maximum values of simple and multiple eigenfrequencies and frequency gaps, Struct. Multidiscip. Optim. 34 (2007) 91–110.
[17] J.K. Guest, J.H. Prvost, T. Belytschko, Achieving minimum length scale in topology optimization using nodal design variables, Int J. Numer. Methods Eng. 61 (2) (2004) 238–254.
[18] A. Kawamoto, T. Matsumori, S. Yamasaki, T. Nomura, T. Kondoh, Heaviside projection based topology optimization by a PDE-filtered scalar function, Struct. Multidiscip. Optim. 44 (1) (2011) 19–24.
[19] O. Sigmund, Morphology-based black and white filters for topology optimization, Struct. Multidiscip. Optim. 33 (4–5) (2007) 401–424.
[20] F. Wang, B.S. Lazarov, O. Sigmund, On projection methods, convergence and robust formulations in topology optimization, Struct. Multidiscip. Optim. 43 (6) (2011) 767–784.
[21] G. Allaire, F. Jouve, A.M. Toader, Structural optimization using sensitivity analysis and a level-set method, J. Comput. Phys. 194 (2004) 363–393.
[22] N. Jenkins, K. Maute, An immersed boundary approach for shape and topology optimization of stationary fluid-structure interaction problems, Struct. Multidiscip. Optim. 54 (2016) 1191–1208.
[23] R. Sivapuram, P.D. Dunning, H.A. Kim, Simultaneous material and structural optimization by multiscale topology optimization, Struct. Multidiscip. Optim. 54 (2016) 1267–1281.
[24] A.N. Christiansen, M.N. gensen Jr., , N. Aage, O. Sigmund, J.A. Baerentzen, Topology optimization using an explicit interface representation, Struct. Multidiscip. Optim. 49 (2014) 387–399.
[25] Y.M. Xie, X. Huang, Evolutionary Topology Optimization of Continuum Structures: Methods and Applications, first ed., John Wiley & Sons, Ltd, West Sussex, 2010.
[26] Y.M. Xie, G.P. Steven, A simple evolutionary procedure for structural optimization, Comput. Struct. 49 (1993) 885–896.
[27] D.J. Munk, G.A. Vio, G.P. Steven, Topology and shape optimization methods using evolutionary algorithms: a review, Struct. Multidiscip. Optim. 52 (2015) 613–631.
[28] L. Xia, Q. Xia, X. Huang, Y.M. Xie, Bi-directional evolutionary structural optimization on advanced structures and materials: a comprehensive review, Archiv. Comput. Methods Eng. (2016) 1–42.
[29] X. Huang, Y.M. Xie, Topology optimization of nonlinear structures under displacement loading, Eng. Struct. 30 (2008) 2057–2068.
[30] X. Huang, Z.H. Zuo, Y.M. Xie, Evolutionary topological optimization of vibrating continuum structures for natural frequencies, Comput. Struct. 88 (2010) 357–364.
[31] R. Picelli, W.M. Vicente, R. Pavanello, Y.M. Xie, Evolutionary topology optimization for natural frequency maximization problems considering acoustic-structure interaction, Finite Elem. Anal. Des. 106 (2015) 56–64.
[32] Y.M. Xie, X. Yang, J. Shen, X. Yan, A. Ghaedizadeh, J. Rong, X. Huang, S. Zhou, Designing orthotropic materials for negative or zero compressibility, Int. J. Solids Struct. 51 (2014) 4038–4051.
[33] L. Xia, P. Breitkopf, Concurrent topology optimization design of material and structure within nonlinear multiscale analysis framework, Comput. Methods Appl. Mech. Eng. 278 (2014) 524–542.
[34] L. Xia, P. Breitkopf, Multiscale structural topology optimization with an approximate constitutive model for local material microstructure, Comput. Methods Appl. Mech. Eng. 286 (2015) 147–167.
[35] B. Xu, X. Huang, S. Zhou, Y. Xie, Concurrent topological design of composite thermoelastic macrostructure and microstructure with multi-phase material for maximum stiffness, Compos. Struct. 150 (2016) 84–102.
[36] W.M. Vicente, Z.H. Zuo, R. Pavanello, T.K.L. Calixto, R. Picelli, Y.M. Xie, Concurrent topology optimization for minimizing frequency responses of two-level hierarchical structures, Comput. Methods Appl. Mech. Eng. 301 (2016) 116–136.
[37] X. Wang, S. Xu, S. Zhou, W. Xu, M. Leary, P. Choong, M. Qian, M. Brandt, Y.M. Xie, Topological design and additive manufacturing of porous metals for bone scaffolds and orthopaedic implants: a review, Biomaterials 83 (2016) 127–141.
[38] W.M. Vicente, R. Picelli, R. Pavanello, Y.M. Xie, Topology optimization of frequency responses of fluid-structure interaction systems, Finite Elem. Anal. Des. 98 (2015) 1–13.
[39] R. Picelli, R. van Dijk, W. Vicente, R. Pavanello, M. Langelaar, F. van Keulen, Topology optimization for submerged buoyant structures, Eng. Optim. 49 (1) (2017) 1–21.
[40] K. Svanberg, M. Werme, Sequential integer programming methods for stress constrained topology optimization, Struct. Multidiscip. Optim. 34 (2007) 277–299.
[41] J.W. Duda, M.J. Jakiela, Generation and classification of structural topologies with genetic algorithm speciation, J. Mech. Des. 119 (1997) 127–131.
[42] D. Guirguis, M.F. Aly, A derivative-free level-set method for topology optimization, Finite Elem. Anal. Des. 120 (2016) 41–56.
[43] R. Picelli, W.M. Vicente, R. Pavanello, Evolutionary topology optimization for structural compliance minimization considering design-dependent FSI loads, Finite Elem. Anal. Des. 135 (Supplement C) (2017) 44–55, https://doi.org/10.1016/j.finel.2017.07.005 ISSN 0168-874X.
[44] H. Guan, Y.J. Chen, Y.C. Loo, Y.M. Xie, G.P. Steven, Bridge topology optimisation with stress, displacement and frequency constraints, Comput. Struct. 81 (3) (2003) 131–145, https://doi.org/10.1016/S0045-7949(02)\ignorespaces00440–00446 ISSN 0045-7949.
[45] R.E. Griffith, R.A. Stewart, A nonlinear programming technique for the optimization of continuous processing system, Manag. Sci. 7 (1961) 379–392.
[46] K. Svanberg, The method of moving asymptotes - a new method for structural optimization, Int. J. Numer. Methods Eng. 24 (1987) 359–373.
[47] J. Nocedal, S.J. Wright, Numerical Optimization, second ed. edn, 2006.
[48] P. Dunning, H.A. Kim, Introducing the sequential linear programming level-set method for topology optimization, Struct. Multidiscip. Optim. 51 (2015) 631–643.
[49] H.P. Williams, Integer Programming, Logic and Integer Programming, Springer US, Boston, MA, 2009.
[50] MathWorks, Intlinprog Documentation, 2017. https://www.mathworks.com/help/optim/ug/intlinprog.html[Accessed 30 June 2017].
[51] R. Picelli, W.M. Vicente, R. Pavanello, Bi-directional evolutionary structural optimization for design-dependent fluid pressure loading problems, Eng. Optim. 47 (10) (2015) 1324–1342.
[52] D.J. Munk, G.A. Vio, G.P. Steven, A Bi-directional Evolutionary Structural Optimisation algorithm with an added connectivity constraint, Finite Elem. Anal. Des. 131 (Supplement C) (2017) 25–42, https://doi.org/10.1016/j.finel.2017.03.005 ISSN 0168-874X.
[53] X. Huang, Y.M. Xie, Evolutionary topology optimization of continuum structures with an additional displacement constraint, Struct. Multidiscip. Optim. 40 (2010) 409–416.